Check for updates

ARTICLE

Characterization of DREADD receptor expression and function in rhesus macaques trained to discriminate ethanol

Daicia C. Allen[1,2], Vanessa A. Jimenez[1], Timothy L. Carlson[1], Nicole A. Walter[1], Kathleen A. Grant [1] and Verginia C. Cuzon Carlson [1]✉

Circuit manipulation has been a staple technique in neuroscience to identify how the brain functions to control complex behaviors. Chemogenetics, including designer receptors exclusively activated by designer drugs (DREADDs), have proven to be a powerful tool for the reversible modulation of discrete brain circuitry without the need for implantable devices, thereby making them especially useful in awake and unrestrained animals. This study used a DREADD approach to query the role of the nucleus accumbens (NAc) in mediating the interoceptive effects of 1.0 g/kg ethanol (i.g.) in rhesus monkeys ($n = 7$) using a drug discrimination procedure. After training, stereotaxic surgery was performed to introduce an AAV carrying the human muscarinic 4 receptor DREADD (hM4Di) bilaterally into the NAc. The hypothesis was that decreasing the output of the NAc by activation of hM4Di with the DREADD actuator, clozapine-n-oxide (CNO), would potentiate the discriminative stimulus effect of ethanol (i.e., a leftward shift the ethanol dose discrimination curve). The results showed individual variability shifts of the ethanol dose-response determination under DREADD activation. Characterization of the expression and function of hM4Di with MRI, immunohistochemical, and electrophysiological techniques found the selectivity of NAc transduction was proportional to behavioral effect. Specifically, the proportion of hM4Di expression restricted to the NAc was associated with the potency of the discriminative stimulus effects of ethanol. Together, these experiments highlight the NAc in mediating the interoceptive effects of ethanol, provide a framework for validation of chemogenetic tools in primates, and underscore the importance of robust within-subjects examination of DREADD expression for interpretation of behavioral findings.

INTRODUCTION

Recent advances in chemogenetic tools have resulted in elegant experimental strategies where circuitry can be specifically, repeatedly and reversibly manipulated in awake behaving animals. Chemogenetics encompasses a range of tools in which an engineered small molecule ligand or "actuator" can selectively bind to genetically-modified ion channels or receptors to modulate the activity of neuronal circuits [1–4]. One of the most widely used chemogenetic techniques are Designer Receptors Exclusively Activated by Designer Drugs (DREADDs). DREADDs are mutated muscarinic receptors that have lost their affinity for their endogenous ligand, acetylcholine, and are instead activated by an exogenous actuator [3–6]. Importantly, the designer actuators are intended to be biologically inert and peripherally bioavailable, allowing for reversible manipulation of specific cell populations without the need for repeated intracranial injections [5, 7–11].

DREADDs, particularly in the striatum and amygdala, have been applied to help map neural circuitry underlying animal models of addiction [12, 13]. In models of sensitization to the locomotor effects of alcohol [12] or self-administration [14–17] the striatum has been a primary target. Activation of inhibitory DREADDs in the dorsal or ventral striatum decreases alcohol intake [14–16]. One intriguing aspect of DREADDs is that the principles of receptor

pharmacology apply, such that manipulation of a behavioral output should be sensitive to the exogenous ligand (i.e., ethanol) in a dose-related manner. Drug discrimination is a reliable behavioral pharmacology assay that is used to characterize the receptor basis of a drug's interoceptive (i.e., discriminative stimulus) effects. This approach has been widely used to identify the receptor basis of ethanol's dose-dependent stimulus effects, particularly in rodents and non-human primates (NHPs) [18–25]. However, the underlying circuitry that mediates the interoceptive effects of ethanol has not been extensively studied. Ethanol produces a mixed, or compound, stimulus that is composed of GABA$_A$ positive modulation and NMDA antagonism [18, 20, 21, 26]. There is some direct evidence from rodent studies that the nucleus accumbens (NAc), in particular the NAc core is involved in ethanol's discriminative stimulus effects, with both GABAergic and NMDA glutamatergic mechanisms shown by intra-accumbens injections of ethanol, neurosteroids, benzodiazepines and phencyclidine [27–31]. In addition, in humans, subjective ratings have strongly implicated the ventral striatum in subjective ethanol intoxication [32–34]. Ethanol acting as both a GABA$_A$ positive modulator and a NMDA antagonist within the NAc would be expected to have a net decrease in the activity of GABAergic projection neurons, disinhibiting target regions. Therefore, if the

NAc is mediating the stimulus effects of ethanol, then inhibition of NAc neurons directly would be additive with the inhibitory effect of ethanol alone, potentiating the ethanol cue (lower ED_{50}).

In the current study, activation of DREADD receptors consisting of the mutated human muscarinic 4 G_i-protein coupled-receptor (hM4Di) virally expressed within the NAc was used to assess the role of the NAc in ethanol drug discrimination (1.0 g/kg, i.g. vs. water). Utilization of drug discrimination with DREADDs in NHPs enabled the examination of specific ethanol dose-dependent effects of hM4Di activation, as well as non-specific effects on behavior (e.g., response rates). Steps for validation in vivo and post-hoc (i.e., ex vivo) are described as a roadmap for DREADD receptor validation in NHPs.

MATERIALS AND METHODS
Experimental subjects
Seven adult male rhesus macaques (*Macaca mullata*) aged 5–6 years were used in this study. The details of the housing conditions as well as food and water access have been published [26]. All procedures were conducted in accordance with the Guide for the Care and Use of Laboratory Animals and approved by the Oregon National Primate Research Center (ONPRC) Institutional Animal Care and Use Committee.

Viral constructs
The AAV1-hSyn-hM4Di-mCherry virus was diluted to $1e^{12}$ viral genomes/ microliter in AAV storage buffer and stored at $-80\,°C$ until use. Immediately prior to surgery, a gadolinium-based contrast dye (Prohance, 0.2 mM) was added to the virus to allow for visualization of the injection site after surgery. The viral mixture was kept on ice and away from light until injection. Additional details can be found in the Supplementary Methods.

MRI-guided stereotaxic surgery
Monkeys were sedated with ketamine (10 mg/kg, i.m.), transported to the magnetic resonance imaging (MRI) suite, intubated, and placed in an MRI-compatible stereotaxic frame. T1-weighted MR images were collected for individual determination of coordinates targeting the bilateral NAc. After the scan, monkeys were transported to the surgical suite and prepped for surgery. One deposit of the viral mixture (30–50 µl) was injected into the NAc of each hemisphere. Following surgery, monkeys underwent an additional MRI to visualize the injection location by Prohance contrast. Monkeys were maintained on isoflurane (1–3%) throughout both MRIs and surgery. Recovery over a minimum of 7 days occurred prior to resuming behavioral testing. Additional details are provided in Supplementary Methods.

Drug discrimination training and testing with hM4Di activation
Prior to surgery monkeys were trained on a two-choice 1.0 g/kg ethanol (i.g.) vs. water discrimination with a 60 min pre-treatment interval and run through a series of substitution tests that was published previously [26]. Additional information is provided in Supplementary Methods. Criteria was defined as ≥90% of total responding and ≥70% of the first FR responses were on the condition-appropriate lever for five consecutive sessions.

Following surgery, discrimination training resumed until discrimination criteria was reestablished. Ethanol dose (0.0–1.5 g/kg) response determinations without CNO were then conducted. Intermediate doses (0.25–0.5 g/kg) were double-determined, counter-balanced for the training session on the day prior (water or ethanol). These dose response curves served as "baseline" for hM4Di-activation comparisons.

After a minimum of 4 weeks, hM4Di-activation during discrimination testing began. The initial dose of CNO used was 5.6 mg/kg (i.m.) for all subjects, which corresponded to plasma concentrations of CNO above 1.0 µg/ ml during the test sessions [35]. If a rate decreasing effect was observed, the dose of CNO was decreased and similarly if no effect was observed the dose of CNO was increased up to 10 mg/kg. All tests with CNO and ethanol combinations were double determined. When appropriate, at the end of test sessions, blood samples were collected for CNO and/or BEC assay (1–2 ml). Additional details provided in Supplementary Methods.

Necropsy and tissue collection
At the end of the behavioral experiments (8–10 months after hM4Di surgery), monkeys were sedated with ketamine (15 mg/kg, i.m.) and

transported to the necropsy suite where an overdose of Nembutal (25 mg/ kg, i.v.) was administered. Animals were perfused and brains were collected and sectioned into 4–6 mm coronal blocks based on MRI images as previously described [36, 37].

Whole-cell patch clamp electrophysiology
Coronal brain blocks containing the NAc or VP were sectioned 250 µm thick and prepared for current and voltage clamp experiments. For all experiments, individual putative neurons were identified as hM4Di expressing or not based on mCherry fluorescence. During current clamp experiments, neurons were current-clamped at 0 pA and membrane potentials and action potentials were recorded during 250 ms sweeps of hyperpolarizing steps from $-100\,pA$ and progressively depolarizing to $+200\,pA$ before, during and after bath application of CNO (500 nM). During voltage clamp experiments, neurons were held at $-60\,mV$. Spontaneous inhibitory postsynaptic currents (sIPSCs) were detected before, during and after bath application of 250 or 500 nM CNO (concentrations based on [35]). Additional details in Supplementary Methods.

Immunohistochemistry
Following tissue collection for electrophysiology, the remaining brain blocks were stored in fresh 4% paraformaldehyde for 48 h. Thin (40 µm) sections were collected using a sliding microtome (Thermo Scientific HM-430) and immunostained for mCherry visualization. Additional details are available in Supplementary Methods.

All images were acquired using a Leica Aperio AT2 400 slide scanner and captured using Aperio eSlide Manager. Using NIH ImageJ (Schneider et al., 2012) a rectangle was placed around the borders of DAB staining to estimate the distance the M-L and D-V spread. In addition, area of expression was determined by drawing a shape around the mCherry-immunopositive fibers and cell bodies and calculated by Image J. The A-P spread was estimated by the number of sections in which mCherry-immunopositive staining was found multiplied by the distance between sections. mCherry-immunopositive area and cell body counts are represented as the mean per section for each individual.

Data analysis
For comparison of ethanol substitution profiles in the presence and absence of CNO, paired *t* tests of ED_{50} values were conducted. Response rates were analyzed using two-way repeated measures mixed effects models. All analysis was conducted using GraphPad Prism 9 or R (version 3.1.2). Data were expressed as mean ± SEM.

Correlations between the CNO-induced percent change in ED_{50} and post-hoc measurements were performed using Prism Version 9.1.0. The Pearson correlation coefficient was reported and significance is determined as $p < 0.05$.

RESULTS
Manipulation of inhibitory DREADD receptors in drug discrimination
Before surgery, CNO (10 mg/kg, i.m.) was tested during ethanol discrimination in combination with training drugs, water ($n = 5$) and 1.0 g/kg ethanol ($n = 2$). There were no significant effects on ethanol-appropriate responding (CNO + water: $t(4) = 0.88$, $p = 0.42$; CNO + Ethanol: $t(1) = 1.00$, $p = 0.5$; Supplementary Fig. 1a) or response rate (CNO + water: $t(4) = 1.82$, $p = 0.14$; CNO + Ethanol: $t(1) = 0.67$, $p = 0.62$; Supplementary Fig. 1b). Following hM4Di injection targeting the bilateral NAc, ethanol dose response curves were determined in the absence of CNO and serve as the "baseline" for our studies (ED_{50}: $0.59 ± 0.06$ g/kg) (Fig. 1a–c). Subsequently, after 4+ weeks for viral expression, CNO was administered 30 min prior to ethanol or water (i.g.) during test sessions. All subjects, except Monkey 2, were tested with 5.6 mg/kg CNO. For Monkey 2, 1.7 mg/kg CNO was used, as 3.0 and 5.6 mg/kg CNO produced rate decreasing effects that were not present prior to surgery.

Activation of hM4Di in the NAc by CNO did not have a consistent effect on mean ethanol dose-response curves ($F(1, 6) = 0.04$, $p = 0.84$) or ED_{50} (+ CNO ED_{50}: $0.54 ± 0.12$ g/kg; $t(6) = 0.28$;
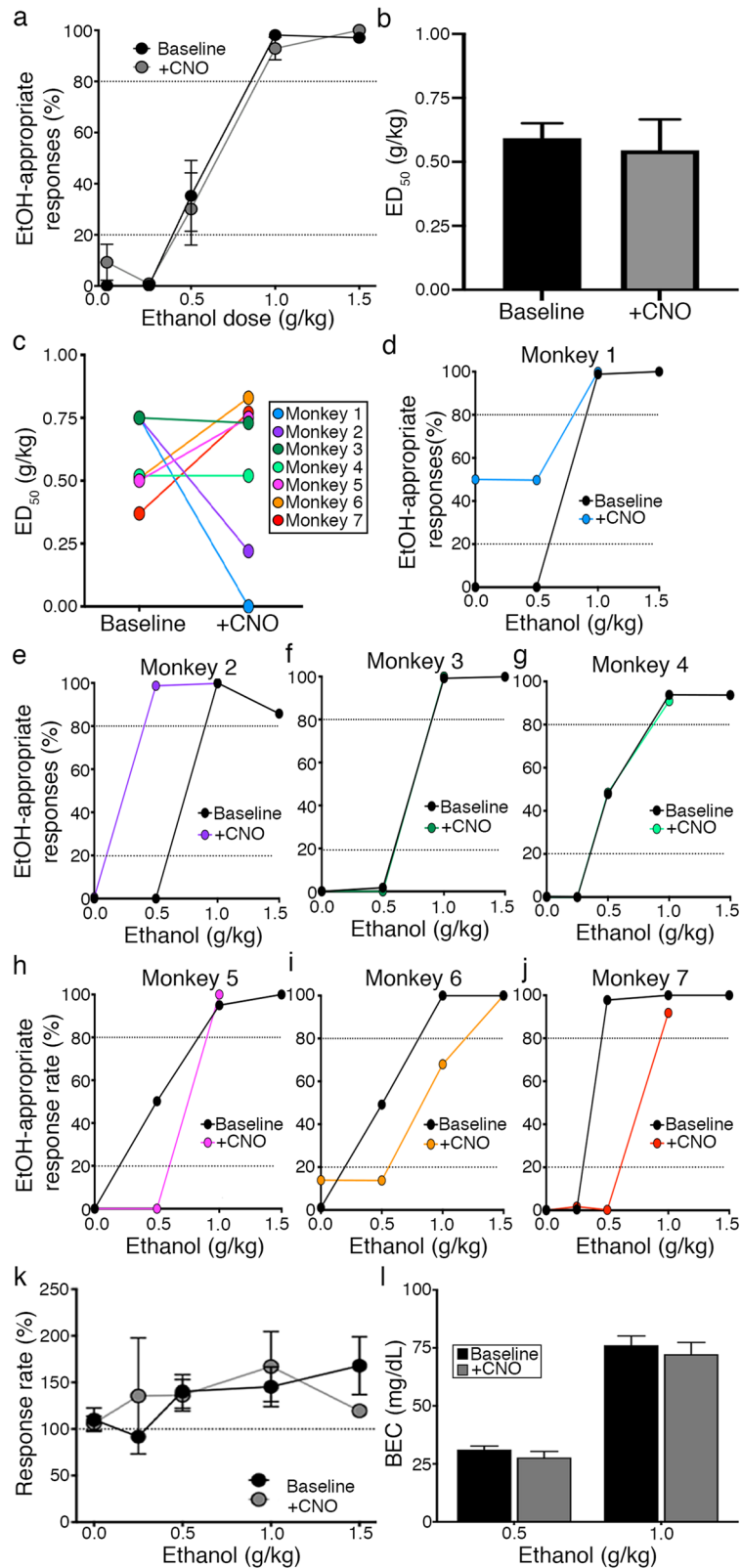
Fig. 1 Ethanol drug discrimination following bilateral activation of hM4Di DREADDs. a Ethanol dose response curves during baseline (black) and following administration of CNO to activate hM4Di receptors (gray). **b** Average ED_{50} during baseline (black) and in the presence of CNO (gray). **c** ED_{50} calculated from ethanol dose response curves for each subject at baseline and in the presence of CNO (5.6 mg/kg for all subjects except Monkey 2 (1.7 m/kg), see "Methods"). **d–j** Individual mean dose response curves during baseline and in the presence of CNO for each monkey. **k** Average response rate at each ethanol dose at baseline (black) and following CNO (gray). **l** BECs at baseline and after CNO taken at the end of 0.5 g/kg or 1.0 g/kg ethanol test sessions. Data are expressed as mean ± SEM.
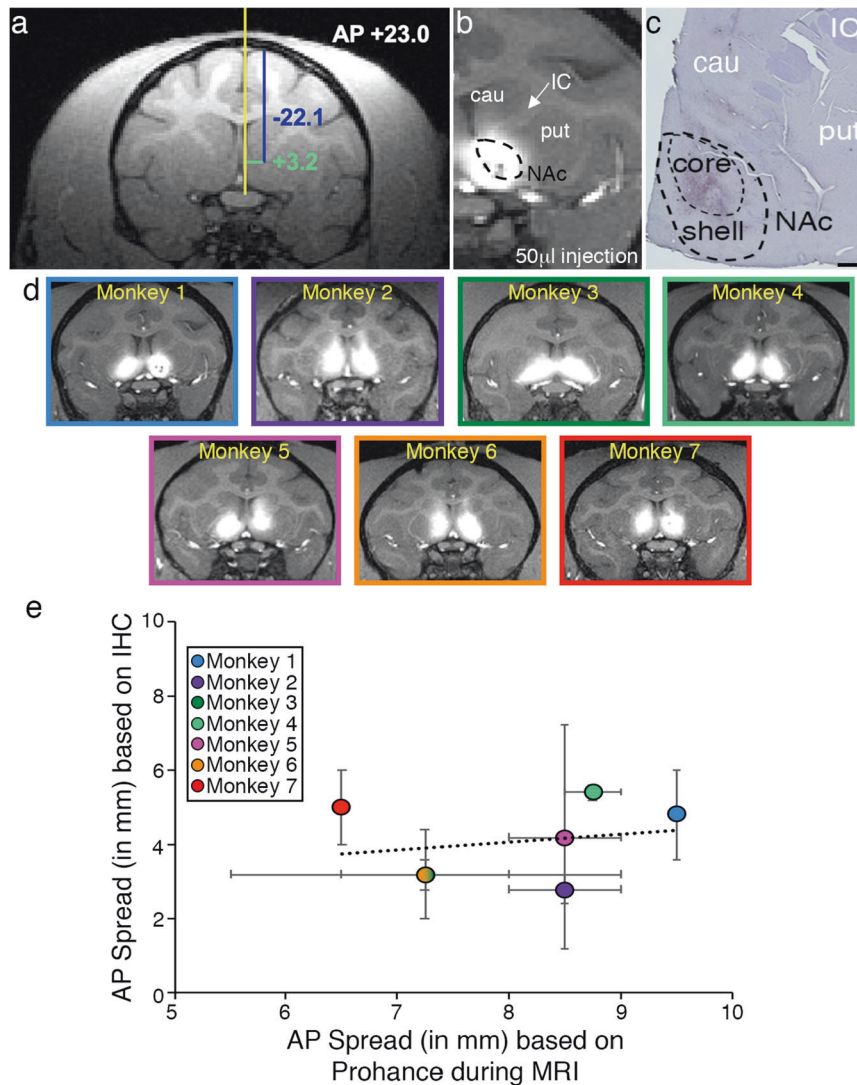
Fig. 2 Localization of DREADD injection using contrast MRI does not correlate with virus transduction. a Representative structural MR image to determine stereotaxic surgery coordinates targeting the dorsal end of the NAc core. Midline at the sagittal sinus shown in yellow. AP coordinate determined from ear bars. ML coordinate in green, DV coordinate in blue. **b** MR image along the coronal plane of individual monkey (Monkey 1) taken directly after stereotaxic surgery (cau caudate, put putamen, IC internal capsule). **c** Representative image from the same monkey (Monkey 1) showing the dissected region containing the striatum stained with an antibody raised against mCherry and visualized with DAB. **d** The images display the peak intensity of GAD contrast for each subject, which is assumed to reflect the injection plane. **e** Correlation between the presumed spread of the virus along the anterior-posterior axis based on Prohance during MRI versus that based on immunohistochemistry of mCherry ($r = 0.30$, $p = 0.30$). Error bars reflect variance across hemispheres expressed as mean ± SEM.

$p = 0.79$) (Fig. 1a–c). Despite no group differences (Fig. 1b), there was notable individual variance in the response to hM4Di activation (Fig. 1c). In 2/7 monkeys, CNO decreased ED_{50} (Fig. 1d, e). One of these subjects received the lower dose of CNO (Monkey 2), suggesting increased sensitivity in this subject. In 3/7 monkeys, CNO-activation of hM4Di increased ethanol ED_{50} (Fig. 1h–j). The remaining two monkeys had no change in ethanol ED_{50} (Fig. 1f, g). There were no significant hM4Di activation-induced changes in response rates during test sessions ($p = 0.93$; Fig. 1k).

To confirm no metabolic interaction between CNO and ethanol, blood samples were collected at the end of each session. There was no significant effect of CNO on BEC (Fig. 1l; $F(1, 6) = 0.57$, $p = 0.36$) and no interaction between CNO and ethanol doses ($F(1, 6) = 0.004$, $p = 0.95$). There was a main effect of CNO dose on plasma CNO concentration ($F(1, 17) = 21.23$, $p < 0.0005$) but no effect of ethanol dose ($F(2, 17) = 1.16$, $p = 0.34$) (Supplementary Fig. 1c). The variance in ethanol ED_{50} was not related to BEC, as there was no correlation between ethanol-appropriate responding

at an ethanol dose below the training dose (0.5 g/kg) and BEC during hM4Di test sessions ($r = 0.06$, $p = 0.9$).

Examination of DREADD delivery using GAD contrast MRI
In order to characterize the extent of the hM4Di receptor expression within the NAc, several techniques were used. First, Prohance (0.2 mM, gadolinium contrast dye) was added to the virus mixture at the time of infusion, to determine if the Prohance spread at the time of surgery could serve as a proxy for DREADD localization (Fig. 2a, b, d). An individual example is shown in Fig. 2b, c (Monkey 1). Qualitative comparison suggests that the location of Prohance contrast is similar to the location of mCherry immunoexpression post hoc. To determine the relationship between Prohance contrast and mCherry expression, spread along the anterior-posterior (AP) plane was determined by the number of MRI images/sections in which expression was observed multiplied by the distance between images (0.5 mm) or section (40 μm). The whole striatum was included as Prohance contrast
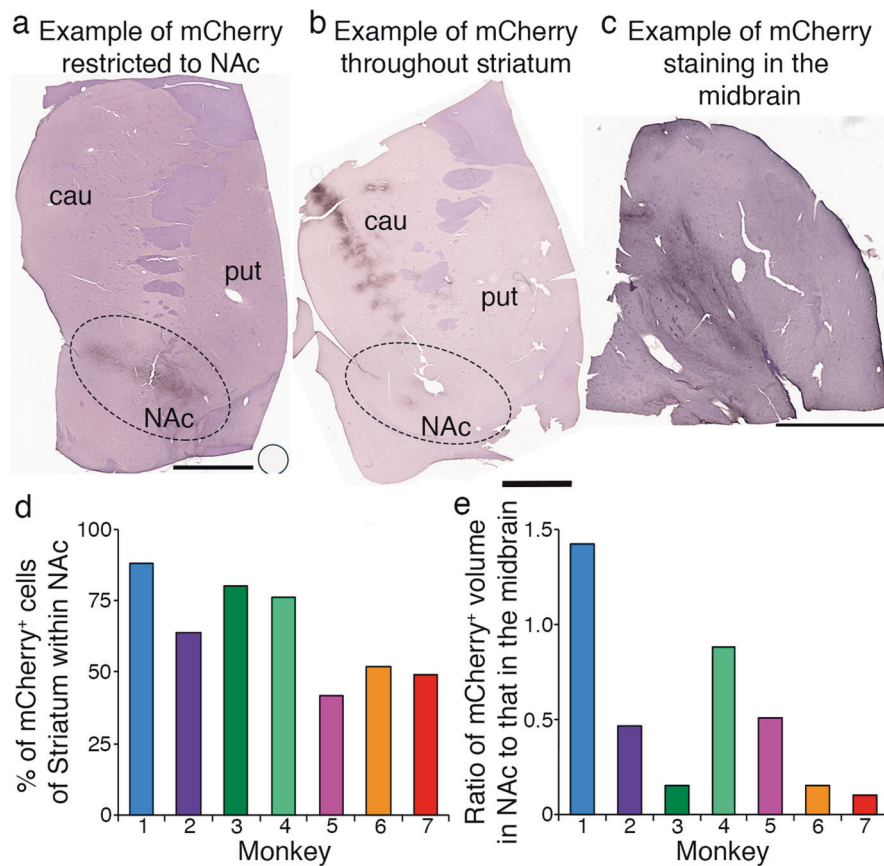
Fig. 3 Immunohistochemical analysis of mCherry to localize DREADD receptors at the level of the striatum and midbrain.
a, **b** Representative image showing the dissected region containing the striatum with an example of mCherry staining restricted to the NAc (**a**) and spread through the overlying caudate (**b**). **c** Representative image at the level of the midbrain showing fiber staining. **d** mCherry+ cell bodies were counted in the striatum and the percentage of cells that were located within the NAc was determined. **e** A ratio of the volume of mCherry immunostaining in the NAc to that in the midbrain. Scale bar in a–c is 3 mm.

and expression often spread beyond the NAc (Fig. 2c, d). The MRI of peak Prohance contrast for each monkey is shown in Fig. 2d. Overall the extent of Prohance spread was greater than mCherry immunostaining in all monkeys (Prohance: 8.04 ± 0.35 mm; mCherry: 4.09 ± 0.46 mm). In addition, the A-P spread of Prohance was not significantly correlated to the A-P spread of mCherry expression within the striatum ($r = 0.30$, $p = 0.30$; Fig. 2e).

Immunohistochemical analysis of DREADD expression in the striatum
In addition to comparing A-P spread of mCherry expression to Prohance MRI, the extent of mCherry expression was quantified for each monkey at the end of the experiment (tissue collected 274.3 ± 10.9 days after surgery). Expression of mCherry at the level of the striatum (Fig. 3a, b) and at the level of the VTA (Fig. 3c), a major output region of the NAc, was determined for each subject. Within sections that contained the striatum, two patterns of staining were observed: mCherry expression restricted to the NAc (Fig. 3a) or mCherry expression located within the NAc and the overlying caudate nucleus (Fig. 3b). Based on previous studies using AAV1 in rhesus monkeys, significant spread across synapses was not predicted [38]. Thus, mCherry-immunopositive cell bodies outside of the NAc may indicate spread of the injection volume to neighboring sites at the time of surgery. To reflect these two patterns, mCherry+ cells were counted throughout the striatum (NAc and caudate) and the percentage of mCherry+ cells that were located within the NAc was calculated (Fig. 3d, range = 41.59–87.72%). The higher the percentage of mCherry+ cells in

the NAc relative to that in the striatum, the more restricted the expression was to the NAc.

Next, midbrain sections that included the VTA and substantia nigra (SN) were examined (Fig. 3c). No primary cell bodies were mCherry+, but there were fibers of passage and outlines of cell bodies potentially depicting mCherry+ terminals from the striatum, consistent with other studies using AAV1 in the striatum [38]. The volume of mCherry staining was measured in the NAc and in the midbrain and the ratio of the mCherry+ volume within the NAc to that within the midbrain was calculated (Fig. 3e, range = 0.11–1.42). Lower values on this scale reflect relatively greater mCherry expression in the midbrain relative to the striatum (Fig. 3e).

Characterizing DREADD receptor function with slice electrophysiology
Using mCherry as a proxy to denote expression of hM4Di, mCherry-positive and mCherry-negative MSNs in the NAc were targeted for current-clamp recordings to measure intrinsic membrane properties and action potential characteristics. MSNs were clamped at 0pA and membrane potentials were recorded following hyperpolarizing and depolarizing current injections in ACSF and then following ACSF supplemented with CNO (200 nM or 500 nM) to activate hM4Di (Fig. 4a). CNO-activation of hM4Di did not alter intrinsic membrane properties such as input resistance (IR, Fig. 4b), capacitance (data not shown), and resting membrane potential (RMP, Fig. 4b) of mCherry-positive cells compared to baseline. However, activation of hM4Di in mCherry-
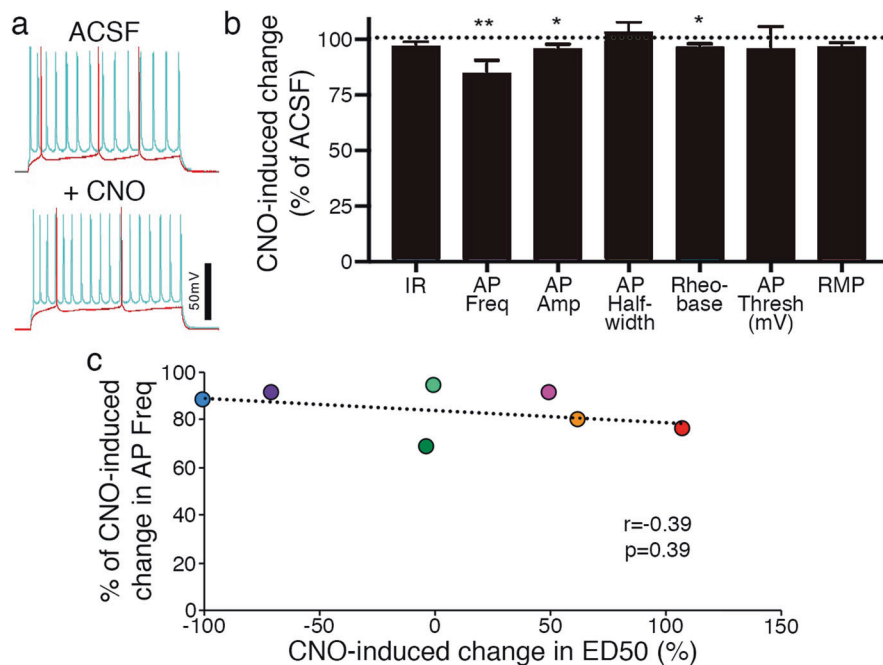
Fig. 4 Ex vivo whole-cell patch clamp electrophysiological analysis of DREADD function. a Representative current clamp recordings from mCherry+ cells located in the NAc taken with injection of depolarizing currents to elicit action potentials in the presence of ACSF (top) and in the presence of CNO (bottom). **b** Percent CNO-induced change from ACSF in membrane and action potential properties. **c** Correlation between CNO-induced change in AP frequency in the NAc and ethanol ED_{50} ($r = 0.39$, $p = 0.39$). Data expressed as mean ± SEM. Paired t test, * < 0.05, ** < 0.01.

positive cells did alter AP characteristics such as decreasing AP frequency and amplitude, as well as the rheobase (Fig. 4b). In the presence of CNO, mCherry-negative cells were not altered in their intrinsic membrane properties or action potential characteristics (data not shown).

Recordings from mCherry-negative VP neurons were used to determine the effect of CNO-activation of hM4Di on GABAergic transmission downstream of the NAc. Comparing VP sIPSCs before and during bath application of CNO (200 nM) showed a significant decrease is sIPSC frequency ($p = 0.0006$), but not sIPSC amplitude ($p = 0.18$), suggesting that activation of hM4Di in the VP decreases the release of GABA (data not shown). Examination of individual monkeys revealed a significant CNO-induced decrease in sIPSC frequency in all monkeys except for Monkey 1 ($p = 0.92$) and Monkey 6 ($p = 0.57$).

Correlation of DREADD function or expression with ethanol discrimination behavior

Last, the behavioral results (CNO-induced changes in ethanol ED_{50}) were correlated with post hoc analyses of mCherry expression and function to determine which best related to individual differences. Functional CNO-induced changes in neuronal activity in the NAc (AP frequency) and VP (sIPSC frequency) did not correlate with changes in ethanol ED_{50} (Fig. 4c; AP frequency: $r = -0.39$, $p = 0.39$; sIPSC: $r = -0.20$, $p = 0.34$, data not shown). The primary measure that correlated with the behavior was the percentage of mCherry staining in the NAc relative to the staining in the whole striatum ($r = -0.82$; $p = 0.023$; Fig. 5a). When the virus expression was more localized to the NAc, hM4Di activation lead to a potentiation of the ethanol discrimination and lower ED_{50}, consistent with our hypothesis (Fig. 5a; example staining in Fig. 3a). In monkeys where virus expression was less restrained to the NAc, hM4Di activation lead to an increase in ethanol ED_{50} (Fig. 5a; example staining in Fig. 3b). This observation is corroborated by the lack of correlation between either mCherry+ dorsal-ventral extent ($r = -0.42$, $p = 0.35$, Supplementary Fig. 2a) or volume within the striatum ($r = 0.18$; $p = 0.70$; Supplementary Fig. 2b) with that of CNO-induced

changes in ED_{50}. However, when these measures are limited to the NAc, then the dorsal-ventral extent ($r = -0.86$, $p = 0.012$; Supplementary Fig. 2c) and volume of mCherry+ stain did correlate with CNO-induced change in ED_{50} ($r = -0.76$; $p = 0.046$; Supplementary Fig. 2d). There was no relationship between mCherry in the striatum and CNO-induced changes in response rate during ethanol ($p = 0.34$) or water test sessions ($p = 0.74$). In addition, there is a trend to a negative correlation between the ratio of the mCherry volume within the NAc to that in the midbrain with CNO-induced change in ED_{50} ($r = -0.72$, $p = 0.068$; Fig. 5b).

DISCUSSION
The data presented here make novel contributions to the fields of alcohol pharmacology and the growing literature using chemogenetics in NHPs [10, 11, 39–45]. This is the first study to directly manipulate the activity of a brain nucleus to alter an interoceptive cue using drug discrimination in primates, representing a significant step forward in our understanding of the ventral striatum in mediating the perception of ethanol's discriminative stimulus effects. Tissue collection 8–10 months after DREADD injection surgery revealed robust function of the receptors in vitro and significant mCherry immunostaining in all subjects, confirming long term behavioral studies with hM4Di receptors are feasible and effective. Further, individual differences in shifts of the dose-response determinations were related to the localization and spread from the target area, helping to refine future approaches and data interpretation using chemogenetics. A key finding was that using MRI-guided stereotactic targeting of the NAc did not prevent spread of hM4Di in the striatum.

The primate NAc is an important nucleus in the subjective effects of ethanol
Past studies have implicated the NAc as a key brain area in the mediation of ethanol's discriminative stimulus effects, prompting the targeting of this nucleus with hM4Di receptors [27, 28, 30, 31, 46, 47]. The hM4Di-mediated inhibition of the
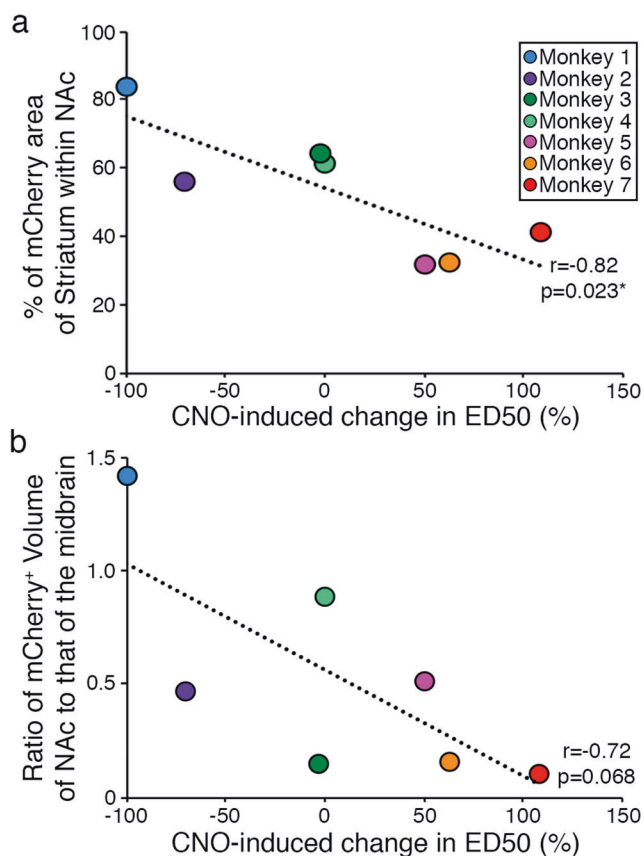
Fig. 5 Correlation between mCherry immunostaining in the NAc-VTA circuit and CNO-induced change in ethanol discrimination. a The percentage of mCherry immunopositive area within the striatum that is localized within the NAc is negatively correlated with the percent change in ED_{50} due to hM4Di activation with CNO ($r = -0.82$, $p = 0.023$). **b** The ratio of the mCherry immunopositive volume within the NAc to that in the VTA trends to a negative correlation with that of the CNO-induced change in ED_{50} ($r = -0.72$, $p = 0.068$).

striatum in the absence of ethanol did not produce full ethanol substitution and there were no changes in ethanol efficacy in any subject, suggesting that the striatum has modulatory effects on 1.0 g/kg ethanol discrimination. Further, the specificity of hM4Di expression in the NAc relative to the whole striatum was related to shifts in ethanol ED_{50} during CNO test sessions (Fig. 5a). The inverse correlation between selectivity of mCherry to the NAc and change in ED_{50} for substitution supports the hypothesis that inhibition of the NAc may potentiate ethanol's discriminative stimulus effects (decreased ED_{50}), consistent with pharmacological manipulations in the rodent [27, 28]. In monkeys where the hM4Di expression spread beyond the NAc to the dorsal striatum, co-inhibition of the NAc and dorsal striatum (primarily caudate) resulted in ethanol antagonism. A key feature of the primate ventral striatum is a more prominent projection to the midbrain, with fewer reciprocal projections from midbrain to the ventral striatum [48]. The trend relationship between midbrain hM4Di expression indicates that higher expression of mCherry in the midbrain relative to the NAc (lower NAc:midbrain mCherry ratio, Fig. 5b) was associated with antagonism of the ethanol cue (increased ED_{50}). This preliminary result may indicate that inhibition of the striatal efferent to the midbrain has an opposing effect on ethanol discrimination. These results may provide support for a hypothesis that afferents to the NAc are more directly involved in ethanol discriminative stimulus effects than efferent projections from the NAc. Further studies are needed to address this hypothesis.

There were two subjects in which there were no effects of CNO administration, suggesting that these subjects may have based their discrimination of ethanol on activity in other brain areas. Alternatively, it is possible that global inhibition of neurotransmission mediated by hM4Di was not pharmacologically similar enough to ethanol, particularly given the high specificity of the ethanol cue in primates [19, 49]. Specifically, in these 7 subjects, $GABA_A$, NMDA, and opiate receptor ligands were previously tested for substitution with the ethanol cue and indicated the basis of the discrimination was pharmacologically specific [26]. Beyond ethanol discrimination, one possible outcome was that chemogenetic inhibition of the NAc would globally disrupt task performance. However, no such deficits were observed, which may reflect an extensive training context, compared to studies on NAc involvement in cue-learning under extinction [50–52] or drug-seeking paradigms [51].

Within-subjects validation of chemogenetics is essential for primate behavioral studies
Examination of hM4Di receptor function through in vitro slice electrophysiology in the same subjects that were included in the behavioral experiments is a key strength of the current study. This is the first report in NHPs to use slice physiology to confirm DREADD activation at concentrations of CNO determined in CSF [35]. These results confirm hM4Di receptor function to decrease spike frequency and action potential amplitude in mCherry-expressing neurons of the NAc, as well as decrease the frequency of downstream sIPSCs in mCherry-negative neurons of the VP. One recent study used in vivo electrophysiology to validate hM4Di receptor activation by local administration of CNO within the external globus pallidus, but no behavioral studies were conducted in conjunction with these recordings [44]. Within-subjects validation is exceedingly important when translating from the rodent to the macaque, particularly given the known genetic and environmental variability of laboratory macaques [53].

In addition to slice recordings, mCherry-immunostaining was examined and the total area of the striatum that expressed mCherry was calculated for each monkey. At the outset of the project, it was unclear which quantitative method would be most reliable in interpretation of the behavioral results. These results highlight that post hoc examination of receptor localization and function is essential for validation of chemogenetic tools in NHPs. Gadolinium contrast MRI was not as informative for determining individual variance in expression and cannot be used as a proxy for characterization of cellular immunostaining. The regional differences in mCherry expression were not predicted by surgical parameters such as total virus volume [40], thus post hoc characterization was critical for interpreting behavioral findings [40, 41].

There are a few known limitations of the current study. The presence of AAV neutralizing antibodies were not determined prior to surgery [54], and the sub-cellular localization of hM4Di receptors was not characterized to determine what percentage of receptors reached the cell surface [43]. In addition, given the extent of expression observed beyond the NAc, hM4Di injection volumes of 30–50 µl were likely too large for the size of the target region. Similar or larger hM4Di injection volumes have been used effectively in larger brain structures like the cortex, though similar differences in the extent of expression were also observed [40].

In conclusion, these experiments provide strong foundational work for an expansion of chemogenetics in dissecting the circuitry mediating complex behaviors in NHPs. The choice of a drug discrimination procedure allowed dose-related changes in the detection of ethanol to be evaluated and quantified. Shifts in the ED_{50} of ethanol provide a pharmacological assay to gauge the effectiveness of a receptor-based manipulation such as hM4Di activation. As the field progresses, with the development of more selective actuator ligands [10, 11, 42] and new chemogenetic tools

such as pharmacologically selective actuator module/pharmacologically selective effector molecules (PSAM/PSEM), there is significant potential to unveil new translational findings in NHPs in an effort to better understand alcohol pharmacology and addiction. In addition, application of non-invasive imaging techniques [10, 11, 45] will allow for expansion of the utility of chemogenetics in NHPs. With these new tools, continuing to maintain a high standard of validation of DREADDs in all subjects and use of robust within-subject experimental designs is of utmost importance. This is particularly true as chemogenetics are applied to more complex alcohol-related behaviors, such as self-administration and response to alcohol withdrawal, in which changes following chemogenetic manipulations may be more challenging to isolate.

REFERENCES

1. Farrell MS, Roth BL. Pharmacosynthetics: reimagining the pharmacogenetic approach. Brain Res. 2013;1511:6–20.
2. Sternson SM, Roth BL. Chemogenetic tools to interrogate brain functions. Annu Rev Neurosci. 2014;37:387–407.
3. Urban DJ, Roth BL. DREADDs (designer receptors exclusively activated by designer drugs): chemogenetic tools with therapeutic utility. Annu Rev Pharm Toxicol. 2015;55:399–417.
4. Roth BL. DREADDs for Neuroscientists. Neuron. 2016;89:683–94.
5. Armbruster BN, Li X, Pausch MH, Herlitze S, Roth BL. Evolving the lock to fit the key to create a family of G protein-coupled receptors potently activated by an inert ligand. Proc Natl Acad Sci. 2007;104:5163–8.
6. Lee H-M, Giguere PM, Roth BL. DREADDs: novel tools for drug discovery and development. Drug Disco Today. 2014;19:469–73.
7. Chen X, Choo H, Huang X-P, Yang X, Stone O, Roth BL, et al. The first structure-activity relationship studies for designer receptors exclusively activated by designer drugs. ACS Chem Neurosci. 2015;6:476–84.
8. Vardy E, Robinson JE, Li C, Olsen RHJ, DiBerto JF, Giguere PM, et al. A new DREADD facilitates the multiplexed chemogenetic interrogation of behavior. Neuron. 2015;86:936–46.
9. Thompson KJ, Khajehali E, Bradley SJ, Navarrete JS, Huang XP, Slocum S, et al. DREADD agonist 21 is an effective agonist for muscarinic-based DREADDs in vitro and in vivo. ACS Pharm Transl Sci. 2018;1:61–72.
10. Nagai Y, Miyakawa N, Takuwa H, Hori Y, Oyama K, Ji B, et al. Deschloroclozapine, a potent and selective chemogenetic actuator enables rapid neuronal and behavioral modulations in mice and monkeys. Nat Neurosci. 2020;23:1157–67.
11. Bonaventura J, Eldridge MAG, Hu F, Gomez JL, Sanchez-Soto M, Abramyan AM, et al. High-potency ligands for DREADD imaging and activation in rodents and monkeys. Nat Commun. 2019;10:4627.
12. Ferguson SM, Neumaier JF. Using DREADDs to investigate addiction behaviors. Curr Opin Behav Sci. 2015;2:69–72.
13. Yager LM, Garcia AF, Wunsch AM, Ferguson SM. The ins and outs of the striatum: role in drug addiction. Neuroscience. 2015;301:529–41.
14. Robins MT, Chiang T, Mores KL, Alongkronrusmee D, van Rijn RM. Critical role for Gi/o-protein activity in the dorsal striatum in the reduction of voluntary alcohol intake in C57Bl/6 mice. Front Psychiatry. 2018;9:112.
15. Cheng Y, Wang J. The use of chemogenetic approaches in alcohol use disorder research and treatment. Alcohol. 2019;74:39–45.
16. Townsley KG, Borrego MB, Ozburn AR. Effects of chemogenetic manipulation of the nucleus accumbens core in male C57BL/6J mice. Alcohol. 2021;91:21–7.
17. Jaramillo AA, Randall PA, Stewart S, Fortino B, Van Voorhies K, Besheer J. Functional role for cortical-striatal circuitry in modulating alcohol self-administration. Neuropharmacology. 2018;130:42–53.
18. Allen DC, Ford MM, Grant KA. Cross-species translational findings in the discriminative stimulus effects of ethanol. In: Porter JH, Prus AJ, editors. The behavioral neuroscience of drug discrimination, Cham: Springer International Publishing; 2018. p. 95–111.
19. Grant KA, Azarov A, Bowen CA, Mirkis S, Purdy RH. Ethanol-like discriminative stimulus effects of the neurosteroid 3 alpha-hydroxy-5 alpha-pregnan-20-one in female Macaca fascicularis monkeys. Psychopharmacol (Berl). 1996;124:340–6.
20. Grant KA, Waters CA, Green-Jordan K, Azarov A, Szeliga KT. Characterization of the discriminative stimulus effects of GABA(A) receptor ligands in Macaca fascicularis monkeys under different ethanol training conditions. Psychopharmacol (Berl). 2000;152:181–8.
21. Vivian JA, Waters CA, Szeliga KT, Jordan K, Grant KA. Characterization of the discriminative stimulus effects of N-methyl- D-aspartate ligands under different ethanol training conditions in the cynomolgus monkey (Macaca fascicularis). Psychopharmacol (Berl). 2002;162:273–81.
22. Grant KA, Colombo G. Discriminative stimulus effects of ethanol: effect of training dose on the substitution of N-methyl-D-aspartate antagonists. J Pharm Exp Ther. 1993;264:1241–7.
23. Grant KA, Colombo G. Substitution of the 5-HT1 agonist trifluoromethylphenylpiperazine (TFMPP) for the discriminative stimulus effects of ethanol: effect of training dose. Psychopharmacol (Berl). 1993;113:26–30.
24. Green KL, Grant KA. Evidence for overshadowing by components of the heterogeneous discriminative stimulus effects of ethanol. Drug Alcohol Depend. 1998;52:149–59.
25. Stolerman IP, Olufsen K. Generalisation of ethanol with drug mixtures containing a positive modulator of the GABA(A) receptor and an NMDA antagonist. Neuropharmacology. 2001;40:123–30.
26. Allen DC, Grant KA. Discriminative stimulus effects and metabolism of ethanol in Rhesus monkeys. Alcohol Clin Exp Res. 2019;43:1909–17.
27. Hodge CW, Alken AS. Discriminative stimulus function of ethanol: role of GABAA receptors in the nucleus accumbens. Alcohol Clin Exp Res. 1996;20:1221–8.
28. Hodge CW, Cox AA. The discriminative stimulus effects of ethanol are mediated by NMDA and GABA(A) receptors in specific limbic brain regions. Psychopharmacol (Berl). 1998;139:95–107.
29. Hodge CW, Nannini MA, Olive MF, Kelley SP, Mehmert KK. Allopregnanolone and pentobarbital infused into the nucleus accumbens substitute for the discriminative stimulus effects of ethanol. Alcohol Clin Exp Res. 2001;25:1441–7.
30. Besheer J, Cox AA, Hodge CW. Coregulation of ethanol discrimination by the nucleus accumbens and amygdala. Alcohol Clin Exp Res. 2003;27:450–6.
31. Besheer J, Schroeder JP, Stevenson RA, Hodge CW. Ethanol-induced alterations of c-Fos immunoreactivity in specific limbic brain regions following ethanol discrimination training. Brain Res. 2008;1232:124–31.
32. Gilman JM, Ramchandani VA, Davis MB, Bjork JM, Hommer DW. Why we like to drink: a functional magnetic resonance imaging study of the rewarding and anxiolytic effects of alcohol. J Neurosci Off J Soc Neurosci. 2008;28:4583–91.
33. Gilman JM, Ramchandani VA, Crouss T, Hommer DW. Subjective and neural responses to intravenous alcohol in young adults with light and heavy drinking patterns. Neuropsychopharmacol Publ Am Coll Neuropsychopharmacol. 2012;37:467–77.
34. Seo D, Sinha R. Chapter 21 - The neurobiology of alcohol craving and relapse. In: Sullivan EV, Pfefferbaum A, editors. Handbook of Clinical Neurology, vol. 125, Elsevier; 2014. p. 355–68.
35. Allen DC, Carlson TL, Xiong Y, Jin J, Grant KA, Carlson VCC. A comparative study of the pharmacokinetics of clozapine N-oxide and clozapine N-oxide hydrochloride salt in Rhesus macaques. J Pharm Exp Ther. 2019;368:199–207.
36. Daunais JB, Kraft RA, Davenport AT, Burnett EJ, Maxey VM, Szeliga KT, et al. MRI-guided dissection of the nonhuman primate brain: a case study. Methods. 2010;50:199–204.
37. Davenport AT, Grant KA, Szeliga KT, Friedman DP, Daunais JB. Standardized method for the harvest of nonhuman primate tissue optimized for multiple modes of analyses. Cell Tissue Bank. 2014;15:99–110.
38. McBride JL, Pitzer MR, Boudreau RL, Dufour B, Hobbs T, Ojeda SR, et al. Preclinical safety of RNAi-mediated HTT suppression in the Rhesus Macaque as a potential therapy for Huntington's Disease. Mol Ther. 2011;19:2152–62.
39. Eldridge MAG, Lerchner W, Saunders RC, Kaneko H, Krausz KW, Gonzalez FJ, et al. Disruption of relative reward value by reversible disconnection of orbitofrontal and rhinal cortex using DREADDs in rhesus monkeys. Nat Neurosci. 2016;19:37–9.
40. Upright NA, Brookshire SW, Schnebelen W, Damatac CG, Hof PR, Browning PGF, et al. Behavioral effect of chemogenetic inhibition is directly related to receptor transduction levels in Rhesus Monkeys. J Neurosci. 2018;38:7969–75.
41. Raper J, Murphy L, Richardson R, Romm Z, Kovacs-Balint Z, Payne C, et al. Chemogenetic inhibition of the amygdala modulates emotional behavior expression in infant Rhesus Monkeys. ENeuro. 2019;6.
42. Upright NA, Baxter MG. Effect of chemogenetic actuator drugs on prefrontal cortex-dependent working memory in nonhuman primates. Neuropsychopharmacology. 2020;45:1793–8.
43. Galvan A, Raper J, Hu X, Paré J-F, Bonaventura J, Richie CT, et al. Ultrastructural localization of DREADDs in monkeys. Eur J Neurosci. 2019;50:2801–13.
44. Deffains M, Nguyen TH, Orignac H, Biendon N, Dovero S, Bezard E, et al. In vivo electrophysiological validation of DREADD-based modulation of pallidal neurons in the non-human primate. Eur J Neurosci. 2021;53:2192–204.
45. Grayson DS, Bliss-Moreau E, Machado CJ, Bennett J, Shen K, Grant KA, et al. The Rhesus monkey connectome predicts disrupted functional networks resulting from pharmacogenetic inactivation of the Amygdala. Neuron. 2016;91:453–66.
46. Jaramillo AA, Randall PA, Frisbee S, Besheer J. Modulation of sensitivity to alcohol by cortical and thalamic brain regions. Eur J Neurosci. 2016;44:2569–80.
47. Jaramillo AA, Agan VE, Makhijani VH, Pedroza S, McElligott ZA, Besheer J. Functional role for suppression of the insular-striatal circuit in modulating interoceptive effects of alcohol. Addict Biol. 2018;23:1020–31.

48. Haber SN, Knutson B. The reward circuit: linking primate anatomy and human imaging. Neuropsychopharmacology. 2010;35:4–26.

49. Helms CM, Rogers LSM, Grant KA. Antagonism of the ethanol-like discriminative stimulus effects of ethanol, pentobarbital, and midazolam in cynomolgus monkeys reveals involvement of specific GABAA receptor subtypes. J Pharm Exp Ther. 2009;331:142–52.

50. Di Ciano P, Everitt BJ. Dissociable effects of antagonism of NMDA and AMPA/KA receptors in the nucleus accumbens core and shell on cocaine-seeking behavior. Neuropsychopharmacology. 2001;25:341–60.

51. Chaudhri N, Sahuque LL, Schairer WW, Janak PH. Separable roles of the nucleus accumbens core and shell in context- and cue-induced alcohol-seeking. Neuropsychopharmacology. 2010;35:783–91.

52. Ambroggi F, Ghazizadeh A, Nicola SM, Fields HL. Roles of nucleus accumbens core and shell in incentive-cue responding and behavioral inhibition. J Neurosci. 2011;31:6820–30.

53. The Macaque Genotype and Phenotype Resource (mGAP). https://mgap.ohsu.edu/. Accessed 9 August 2021.

54. Gray SJ, Nagabhushan Kalburgi S, McCown TJ, Jude, Samulski R. Global CNS gene delivery and evasion of anti-AAV-neutralizing antibodies by intrathecal AAV administration in non-human primates. Gene Ther. 2013;20:450–9.

AUTHOR CONTRIBUTIONS
DCA, KAG, and VCC conceptualized and designed the experiments. DCA, VAJ, NAW, TLC, and VCC collected the data. DCA and VCC analyzed the data. DCA, KAG, and VCC wrote the paper.

COMPETING INTERESTS
The authors declare no competing interests.

ADDITIONAL INFORMATION
Supplementary information The online version contains supplementary material available at https://doi.org/10.1038/s41386-021-01181-5.

Correspondence and requests for materials should be addressed to Verginia C. Cuzon Carlson.

Reprints and permission information is available at http://www.nature.com/reprints

Publisher's note Springer Nature remains neutral with regard to jurisdictional claims in published maps and institutional affiliations.